Title	Tremendous Enhancement of Torque Density in HTS Induction/Synchronous Machine for Transportation Equipments
Author(s)	Nakamura, Taketsune; Itoh, Yoshitaka; Yoshikawa, Masaaki; Nishimura, Tatsuo; Ogasa, Takuro; Amemiya, Naoyuki; Ohashi, Yoshimasa; Fukui, Satoshi; Furuse, Mitsuho
Citation	IEEE Transactions on Applied Superconductivity (2015), 25(3)
Issue Date	2015-06
URL	http://hdl.handle.net/2433/196086
Right	© 2014 IEEE. Personal use of this material is permitted. Permission from IEEE must be obtained for all other uses, in any current or future media, including reprinting/republishing this material for advertising or promotional purposes, creating new collective works, for resale or redistribution to servers or lists, or reuse of any copyrighted component of this work in other works.
Type	Journal Article
Textversion	author

Tremendous Enhancement of Torque Density in HTS Induction/Synchronous Machine for Transportation Equipments

Taketsune Nakamura, Yoshitaka Itoh, Masaaki Yoshikawa, Tatsuo Nishimura, Takuro Ogasa, Naoyuki Amemiya, Yoshimasa Ohashi, Satoshi Fukui, and Mitsuho Furuse

***Abstract*—We succeeded in tremendous enhancement of torque density as well as power density in High Temperature Superconducting Induction/Synchronous Machine (HTS-ISM) for next generation transportation equipments. First, we fabricated and tested the 20 kW-class prototype as the validation of our design concept (1st generation). And then, the 70% reduction of the motor's volume is challenged with the same power (2nd generation). We successfully realized the tremendous enhancement of the torque density, and further the overload tolerance was also realized at the steady state.**

***Index Terms*—HTS, induction/synchronous machine, BSCCO, torque density, transportation equipments**

I. Introduction

OUR PROJECT group has been trying to realize high efficiency power train system for the transportation equipments, e.g., train, bus, truck, automobile, with the use of high temperature superconducting motor. Target motor is so-called High Temperature Superconducting Induction /Synchronous Machine (HTS-ISM) [1]-[6]. Our primary motivation is the realization of the rotor (secondary) windings (Fig. 1) with the use of the HTS conductors (both of rotor bars and end rings are made of the HTS). Advantages of the HTS-ISM are (1) co-existence of synchronous as well as slip modes operation as an intrinsic performance, (2) high efficiency thanks to the steady state synchronous drive, (3) robustness against overload application by switching from the synchronous to the slip mode rotation, (4) tremendous enhancement of the torque density by increasing the current carrying capacity of the HTS windings, (5) autonomous stability against the variable speed control with the help of the nonlinear flux-flow (dissipative) state, etc.

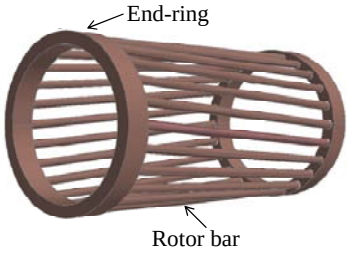

Fig. 1. Schematic diagram of rotor (secondary) windings. Rotor bars are located in the rotor core (silicon steel), and then short-circuited by the end rings [1-6].

Especially, ultimate enhancement of the torque density is one of the most important technological targets for the practical realization of the HTS power train system. That is, the heavy and loss generating transmission gear can be omitted from the system, and this could clarify the superiority of the HTS-ISM drive system to the conventional (normal conducting) one, even we consider the consumed power of the cryocooler.

In this paper, we firstly elucidate the validity of the design code of the motor based on the experiment and the analysis of 1st generation 20 kW motor [6]. Based upon the obtained results, we further fabricate the 2nd generation motor, and then challenge to the 70% reduction in the magnetic volume with the same output power. Through the characteristics comparison between such two motors, we show the possible torque density maximization based on our design.

II. Basic Concept of Synchronous and Slip Mode Rotation of HTS-ISM

Fig. 2 illustrates the schematic diagram of electric field (E) vs. current (I) curve of one rotor bar, and Fig. 3 the corresponding torque (τ) vs. rotational speed (N) curve [7]. Simply speaking, the synchronous rotation mode is realized from the zero resistivity state, and the slip rotation mode from the flux-flow state. In other words, the originality of the HTS-ISM is that not only the zero resistivity state but also the (dissipative) flux-flow state is effectively utilized for the intrinsic rotation mechanism. Especially, the slip rotation mode can be introduced for the short time overload tolerance.

Manuscript received August 12, 2014. This work was supported by Japan Science and Technology Agency's Advanced Low Carbon Technology Research and Development Program (JST-ALCA) in Japan.

T. Nakamura, T. Nishimura, T. Ogasa and N. Amemiya are with Department of Electrical Engineering, Graduate School of Engineering, Kyoto University, 1 Kyoto-Daigaku-Katsura, Nishikyo-Ku, Kyoto 615-8510, Japan (T. Nakamura phone: +81-75-383-2221; fax: +81-75-383-2224; e-mail: tk_naka@kuee.kyoto-u.ac.jp.

Y. Itoh and M. Yoshikawa are with IMRA MATERIAL R&D Co., Ltd, 2-1 Asahi-Machi, Kariya 448-0032, Japan.

Y. Ohashi is with AISIN SEIKI Co., Ltd, 2-1 Asahi-Machi, Kariya 448-0032, Japan.

S. Fukui is with Graduate School of Science and Technology, Niigata University, 8050 Ikarashi-Ninocho, Nishi-Ku, Niigata 950-2181, Japan.

M. Furuse is with National Institute of Advanced Industrial Science and Technology, 1-1-1 Umezono, Tsukuba 305-8568, Japan

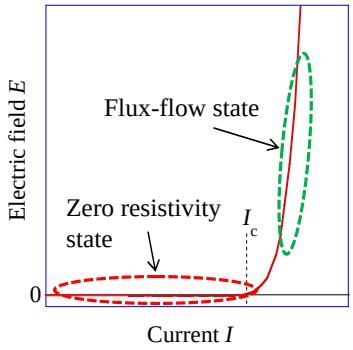

Fig. 2. Schematic diagram of electric field (E) vs. current (I) curve of one rotor bar in the HTS-ISM.

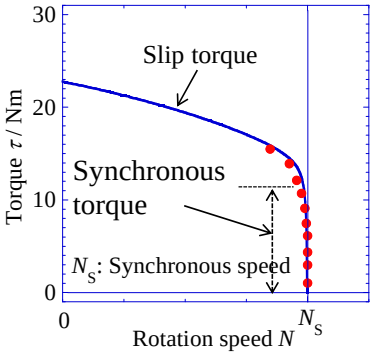

Fig. 3. An example of torque (τ) vs. rotational speed (N) curve [7].

Table I Specifications of 20 kW class HTS-ISM.

	1st generation	2nd generation
Output Power	20 kW	20 kW
Rated voltage	400 V	200 V
Pole number	8	4
Maximum speed	1800 rpm	1800 rpm
Rotor's diameter	159.4 mm	119.3 mm
Stator's diameter	265.0 mm	200.0 mm
Length	200.0 mm	106.0 mm
Gap	0.60 mm	0.35 mm
Magnetic volume	11100 cm^3	3330 cm^3
Weight	83.0 kg	29.6 kg
Critical current of one rotor bar (stack number of BSCCO tapes)	2090 A (11)	1617 A (11)

III. Design and Fabrication of 20 kW Class HTS-ISM

We have designed and fabricated two types of 20 kW class HTS-ISM, and the target power is 20 kW rated synchronous power at 1800 rpm and the liquid nitrogen cooling. Table I shows the specifications of the designed motor. The purpose of the 1st generation motor is the verification of our design technology. Followed by the verification of the characteristics, the 2nd generation motor try to reduce the magnetic volume at 70% with the same power. This also means the 70% increment of the torque density because of the same rotation speed, i.e., 1800 rpm. Further, the pole number (4) and the rated voltage (200 V) of the 2nd generation motor are smaller than that of the 1st generation, i.e., 8 and 400 V (Table I). The critical current of one rotor bar is also different each other, i.e., 2090 A for the 1st generation and 1617 A for the 2nd generation.

Our final target is the fully superconducting HTS motor (both of the stator and the rotor windings are fabricated with HTS conductors). As a first step, the conventional copper

(a) 3-phase, 8-pole Cu stator

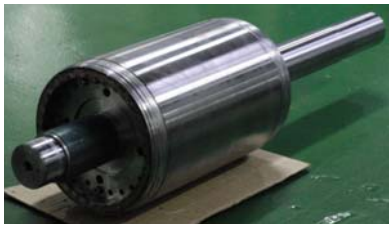

(b) BSCCO rotor

Fig. 4. Photographs of Cu stator and BSCCO rotor in 1st generation 20 kW class HTS-ISM [6].

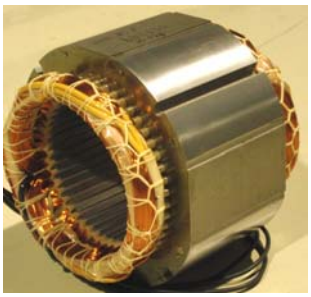

(a) 3-phase, 4-pole Cu stator

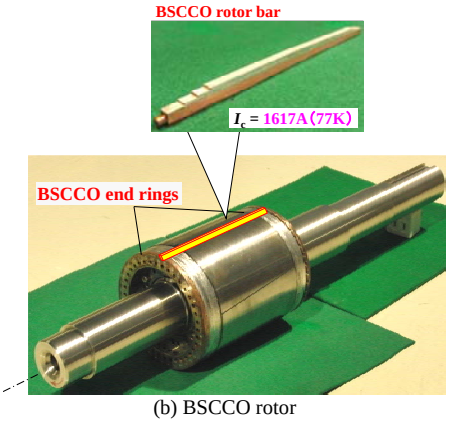

(b) BSCCO rotor

Fig. 5. Photographs of Cu stator and BSCCO rotor in 2nd generation 20 kW class HTS-ISM.

Fig. 6. Photographs of low thermal invasion cryostat for the testing 2nd generation HTS-ISM (Fig. 4).

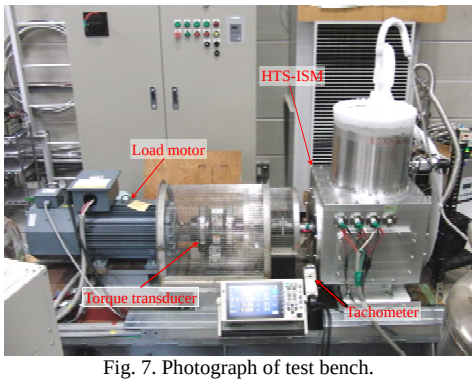

Fig. 7. Photograph of test bench.

stator is utilized, and the HTS rotor is developed in this paper. Firstly, the rough design is carried out through the formulation of the maximum synchronous torque τ_{sm}, which is expressed based on the nonlinear electrical equivalent circuit as follows [1].

$$\tau_{sm} = \frac{P_{sm}}{2\omega / p} = \xi \frac{p}{2} \phi_s' I_c' \quad (1)$$

where, ξ, p, ϕ_s', I_c' and ω, respectively, denote the phase number, the pole number, the air-gap (trapped) magnetic flux, the critical current of one phase and the angular frequency. The superscript ' denotes that the value is converted to the stator (primary) side. The maximum synchronous power P_{sm} is also expressed in the equations. Further, the value of ϕ_s' is formulated as follows.

$$\phi_s' = \frac{\sqrt{V_1^2 - [\omega(l_1 + l_2')I_c']^2} - r_1 I_c'}{\omega} \quad (2)$$

where, V_1, l_1+l_2' and r_1 show the primary phase voltage, the total leakage inductances and the stator resistance, respectively. It should be noted that the I_c' is determined by the average critical current of the BSCCO tapes. Exactly speaking, however, allowable imbalance of such current should be taken into account for the design, and this will be our future works.

The value of P_{sm} is set to be 20 kW in this study, and the corresponding torque τ_{sm} is consistently determined to be 106.1 Nm@1800 rpm. It is noted that the torque is limited by the possible conduction current of the Cu stator and the HTS rotor windings. The balance of such current is important for the design.

Fig. 4 and 5 show the photographs of the 1st generation and 2nd generation HTS-ISM, respectively. It is also noted that the HTS rotor bars are fabricated by stacking BSCCO tapes with the aid of the solder, and then installed in the slots of the rotor core. After such installation is completed, the BSCCO end rings are soldered for both ends of the BSCCO rotor bars [6]. Exactly speaking, therefore, the fabricated squirrel-cage windings possess the joint resistance, and then the estimation of such resistance will be our future work. Fig. 6 shows the low thermal invasion metal cryostat for the testing of the 2nd generation HTS-ISM (Fig. 5).

IV. Test Method

All the tests are executed in atmospheric liquid nitrogen (77 K). Actually, this is not the final cooling method of our motor, but for the verification of the exact characteristics of the fabricated motor. We actually develop the cooling structure with the use of the Stirling-type refrigerator, and this could be reported separately.

Fig. 7 shows a photograph of the test bench. The drive shaft of the fabricated motor is connected to the no-contact torque transducer and the load (permanent magnet) motor. The generated power due to the braking goes back to the HTS-ISM through the free-wheel diodes of the PWM inverter.

V. Results and Discussion

Firstly, the HTS-ISM is pulled in to be the synchronous speed, i.e., 1575 rpm for the 1st generation and 1800 rpm the 2nd generation, and then the generated torque is measured as increasing the load. We have to note that the rotation speed of the 1st generation motor is limited to 1575 rpm because of the inverter's problems, and will carry out the rotation tests at 1800 rpm in near future. The load is applied by means of the commercial permanent magnet motor with constant torque control.

A. First generation HTS-ISM

Fabrication and partial load characteristics have already been reported in our previous paper (Fig. 4) [6], and then the full load test results are only reported in this section. Fig. 8 shows an example of the tested result of the load characteristic. From this figure, we can clearly confirm that the motor's synchronous torque reaches for 20 kW as designed. That is, we can show the integrity of our design technology. It should be noted that the HTS-ISM pulled out against further application of the load, and then this motor does not possess

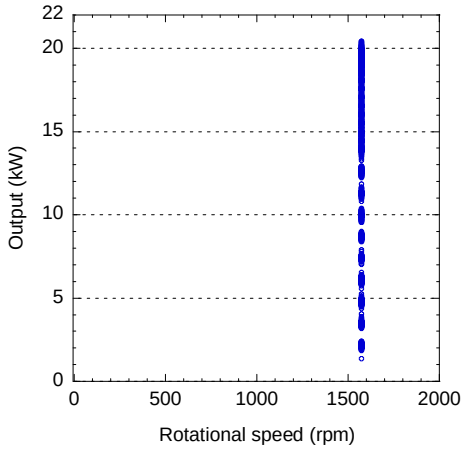

Fig. 8. Example of load test results of 1st generation HTS-ISM.

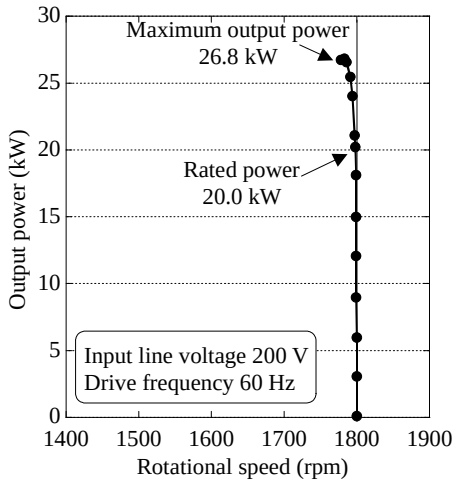

Fig. 9. Example of load test results of 2nd generation HTS-ISM.

any slip mode torque. Main reason is that the leakage reactance is larger in the 1st generation motor.

B. Second generation HTS-ISM

Based on the success of the full load test for the 1st generation HTS-ISM, we further challenge to the enhancement of the torque density. That is, for the 2nd generation HTS-ISM, our target is the 70% reduction in magnetic volume (equivalently, it is almost the same as that of the stator core) with the same power, i.e., 20 kW (Fig. 5).

Fig. 9 shows the load test result at 77 K. As can be clearly seen, the synchronous power reaches for the full load of 20 kW. Moreover, further application of the load (overload) transits the rotation mode of the HTS-ISM from the synchronous to the slip mode, and the slip power reaches for 26.8 kW. Namely, we can realize the overload tolerance with this motor, which concept is usually been introduced for the design of the conventional (normal conducting) motor. It should be noted that the motor volume of this motor is 70% smaller than that of the first generation HTS-ISM, and the corresponding power density is 1.38 kW/kg (this is calculated for the volume of the stator core). From these results, it could be possible to realize the ultimate enhancement of the torque/power density for the next generation power-train system without any loss generating transmission gears.

VI. Conclusion

In this study, we designed, fabricated, and tested the 20 kW class HTS-ISM with the use of BSCCO rotor windings. The BSCCO rotor was coupled with the copper stator, and cooled in liquid nitrogen. Although the magnetic volume of the fabricated (second generation) motor was 70% smaller than that of the first generation one, such motor reached for the same rated power (20 kW) at the rotational speed of 1800 rpm. That is, tremendous enhancement of the torque density as well as the power density can be realized based on our design technology. Actually, the exact value of the efficiency cannot be calculated yet, because the mechanical loss and the viscous loss of the liquid nitrogen are not clear. Then, this estimation will be one of our future works. Also, we will challenge the ultimate maximization of the torque for the realization of the direct-drive power train system.

Acknowledgment

We would like to thank Mr. K. Muranaka and Mr. J. Watanabe at Department of Electrical Engineering, Graduate School of Engineering, Kyoto University, for their partial support of the experiments.

References

[1] G. Morita, T. Nakamura and I. Muta, “Theoretical analysis of a YBCO squirrel-cage type induction motor based on an equivalent circuit,” Supercond. Sci. Technol., vol. 19, pp. 473-478, 2006.

[2] T. Nakamura, Y. Ogama, H. Miyake, K. Nagao and T. Nishimura “Novel rotating characteristics of a squirrel-cage-type HTS induction/synchronous motor,” Supercond. Sci. Technol., vol. 20, pp. 911-918, 2007.

[3] K. Nagao, T. Nakamura, T. Nishimura, Y. Ogama, N. Kashima, S. Nagaya, K. Suzuki, T. Izumi and Y. Shiohara, “Development and fundamental characteristics of a YBCO superconducting induction/synchronous motor operated in liquid nitrogen,” Supercond. Sci. Technol., vol. 21, 015022, 2008.

[4] T. Nakamura, K. Nagao, T. Nishimura, Y. Ogama, M. Kawamoto, T. Okazaki, N. Ayai and H. Oyama, “The direct relationship between output power and current carrying capability of rotor bars in HTS induction/synchronous motor with the use of DI-BSCCO tapes,” Supercond. Sci. Technol., vol. 21, 085006, 2008.

[5] T. Nakamura, K. Matsumura, T. Nishimura, K. Nagao, Y. Yamada, N. Amemiya, Y. Itoh, T. Terazawa and K. Osamura, “A high temperature superconducting induction/synchronous motor with a ten-fold improvement in torque density,” Supercond. Sci. Technol., vol. 24, 015014, 2011.

[6] D. Sekiguchi, T. Nakamura, S. Misawa, H. Kitano, T. Matsuo, N. Amemiya, Y. Itoh, M. Yoshikawa, T. Terazawa, K. Osamura, Y. Ohashi, and N. Okumura, “Trial test of fully HTS induction/synchronous machine for next generation electric vehicle,” IEEE Trans. Appl. Supercond., vol. 22, no. 3, 5200904, 2012.

[7] T. Nakamura, T. Nishimura, K. Nagao, K. Matsumura and Y. Ogama, “Theoretical analysis of high temperature superconducting induction /synchronous machine based on the nonlinear electrical equivalent circuit,” Proc. ICEM'08, ID. 1278 (5pp), 2008.